Reprinted from CLINICAL ORTHOPAEDICS, November, 1996
Volume 332
Lippincott-Raven Publishers Printed in U.S.A.

Bone Injury Response

An Animal Model for Testing Theories of Regulation

Patricia S. Landry, PhD*; Andrew A. Marino, PhD*,**; Kalia K. Sadasivan, MD*; and James A. Albright, MD*

Therapeutic treatment of bone disease and attempts to accelerate normal healing require knowledge of the soluble factors that control bone repair and the specific effects that they produce. To facilitate study of this regulatory system, an animal model involving creation of a hole in the cortex of the rat tibia was developed. Proliferation, differentiation, and callus formation at the injury site were measured more precisely than in previous animal models by means of autoradiographic, histologic, histochemical, and morphometric methods. Several novel features of bone healing were observed, including the following: (1) synthesis of bone matrix in the defect occurred only after a cambial compartment was established by regeneration of the fibrous periosteum and (2) at least 3 kinds of osteoblasts could be distinguished depending on when and where they deposited calcifiable matrix. The model is well suited to evaluating the use of interventional strategies that involve chemical or electrical agents because the cellular parameters of interest can be measured precisely.

From the Departments of *Orthopaedic Surgery and **Cellular Biology and Anatomy, Louisiana State University Medical Center, Shreveport, LA.

Supported in part by a grant from the Hamilton Foundation.

Submitted in partial fulfillment of the degree of Doctor of Philosophy, Department of Cellular Biology and Anatomy, LSUMC (P.S.L.).

Reprint requests to James A. Albright, MD, Department of Orthopaedic Surgery, Louisiana State University Medical Center, PO Box 33932, Shreveport, LA 71130-3932.

Received: September 12, 1995.

Revised: December 6, 1995.

Accepted: January 31, 1996.

The response of bone to trauma consists of a series of specific events that include proliferation of bone stem cells, differentiation into osteoblasts, production of osteoid, mineralization, and modeling. The nature of the healing is influenced by age, extent of injury to hard and soft tissues, type of bone affected, mobility at the fracture site, local pathologic conditions, oxygen levels, products of inflammation, and the mechanical and electrical properties of bone.[5,6,16,22,24] Although this broad outline of the fracture healing response has been known for many years, important questions regarding the means by which the response is controlled and regulated remain unanswered. The lack of such knowledge hampers treatment of some bone diseases and prevents rational extension of empirical observations of beneficial effects caused by exogenous factors.[4,13]

Various animal models have been proposed to facilitate study of the regulatory system governing bone healing,[9,10,15,19,28] and features that may interfere with attempts to isolate the putative role of particular agents

have been identified. Micromotion at the healing site tends to promote cartilage formation that otherwise might not be a concomitant of healing. The presence of fixation devices likewise elicits biologic reactions that are beyond those essential for bone healing. Soft tissue trauma, depending on its nature and extent, might hinder, accelerate, or have no effect on the bone specific events that mediate healing.

An important factor in bone healing that has not been adequately considered in previous animal models is the possible interaction between the regulatory systems governing endosteal and periosteal contributions to bone healing. Trauma can activate the periosteal repair system without affecting the endosteal system, but the converse is not true. Because periosteal healing constitutes the simplest case of regulated osteogenic activity in response to trauma, it is particularly suited to be a model system for studying basic mechanisms.

The current study described and validated a quantitative, reproducible bone injury model in the rat in which the identified perturbing elements were minimized or eliminated. Several novel qualitative observations regarding bone healing have also been described.

METHODS

Animals

Male Fischer rats (Harlan Sprague-Dawley, Indianapolis, IN) were used in all studies; they were caged individually with a light to dark cycle of 12:12 (light commencing at 6:00 a.m.) and fed and watered on demand. The animals were not used until they reached a weight of 200 g (8–10 weeks old), which required a minimum of 1 week from the time of acquisition.

The anteromedial surface of the tibia inferior to the saphenous artery bifurcation was chosen for study because the absence of overlying muscle facilitated analysis of the periosteal response (Fig 1). After an anesthetic was administered (sodium pentobarbital, intraperitoneal, 50 mg/kg), the hind limb was shaved, and a 1.5-cm incision

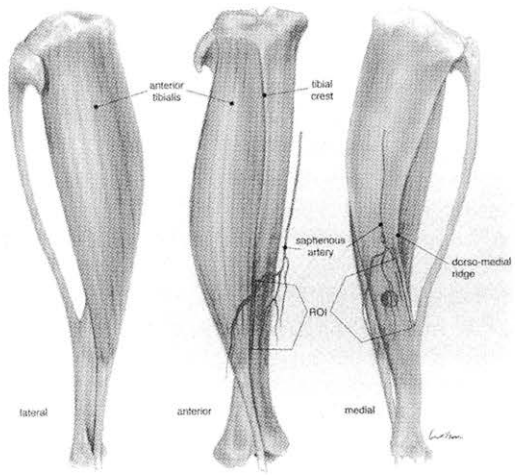

Fig 1. Location of the region of interest (ROI) and the bone defect (blind hole) on the anteromedial surface of the rat tibia.

was made through the skin directly over the tibial crest, with care taken not to injure the underlying bone and adjacent muscle. The superficial fascia was separated from the overlying skin on all sides of the incision, and the skin was retracted to expose the tibia. A defect 0.5-mm deep was created in the center of the region of interest by slowly rotating a hand-operated 1.1-mm jeweler's burr; the depth varied by ±10%, as determined by a depth gauge. To eliminate any influence of the endosteum and marrow on the healing response, care was taken to insure that the defect did not penetrate the medullary cavity. The defect site was washed with saline to remove bone debris, and the skin was closed with sutures.

For qualitative assessment of the healing response, the injury was administered to 56 rats; 8 rats were sacrificed at 1, 2, 3, 5, 7, 14, and 21 days after injury, and the regions of interest were processed by means of 4 different histologic methods. The controls were 8 noninjured rats (16 tibiae) that were otherwise treated the same as the injured animals.

The response of bone to bone injury was studied quantitatively in another group of 30 rats that were sacrificed 1, 2, 3, 5, 7, and 14 days after creation of the bone defect (5 rats at each time interval); 10 noninjured animals (20 tibiae) served as controls. As a positive control for the effect of soft tissue injury, 10% of the lateral most aspect

of the anterior tibialis muscle was removed in 10 rats, with no bone injury; the regions of interest were recovered 2 and 7 days later.

All rats were given tritiated thymidine intraperitoneally 1 hour before sacrifice (1 μCi/g of body weight, diluted with sterile water to a final volume of 0.5 ml, specific activity 2 Ci/mmol; ICN Biomedicals, Irvine, CA). All animal procedures, including operations, radioisotope injections, and euthanasias (carbon dioxide inhalation) were performed between 10:00 a.m. and 2:00 p.m. to minimize potential confounding effects due to circadian rhythms.[12]

Tissue Processing

After sacrifice, the tibiae were resected and excess muscle was cut away, with special care taken not to disturb the anteromedial surface. The proximal epiphysis was removed and the marrow cavity flushed with fixative (10% neutral buffered formalin, 8° C); the tibiae were then fixed, demineralized (Cal-Ex, Fischer Scientific, Pittsburgh, PA, unless noted otherwise), dehydrated, and infiltrated for 2 days in glycol methacrylate (JB-4, except JB-4 Plus in enzyme studies; Polysciences, Warrington, PA). The region of interest was then obtained by cutting the bone transversely 5 and 15 mm distal to the tibial crest notch. The tibial segments were embedded and sectioned completely at 4 μm in the longitudinal plane; every 10th section was mounted on a slide.

In the quantitative study, 9 sections were used for analysis (from 250). A set of 3 sections was selected in each animal from the middle of the defect, from halfway between the middle of the defect and its medial edge, and from halfway between the middle and the lateral edge. One section in each trio was processed for autoradiography and counterstained with van Gieson's, the second was stained with methyl-green/thionin, and the third was stained with toluidine- blue/basic-fuchsin.[2,23]

In the qualitative study, 4 histologic techniques were used (2 rats/technique/day). A general overview of the repair process was obtained with the use of toluidine blue/basic fuchsin. The role of cambial cells was studied by means of alkaline phosphatase localization.[17] A simultaneous coupling dye technique with the use of naphthol AS phosphate as substrate and fast blue BB as the coupler was used to localize alkaline phosphatase.[7] Sections incubated without substrate were used as negative controls; the positive controls were sections of growth plate, kidney, or small intestine.

Osteoclastic resorption was studied by means of tartrate resistant acid phosphatase localization.[17] Localization was achieved by a simultaneous coupling dye method involving hexazotized pararosaniline as the coupler and naphthol AS-TR phosphate as substrate with 10 mM sodium tartrate added to the incubation media.[11] Sections incubated without substrate served as negative controls, and positive controls were sections of growth plate; kidney sections were used as a control for tartrate inhibition. Mineralization was studied by the von Kossa method, with nuclear fast red used as the counterstain.[27] In the tibiae that lacked the bone defect (controls and animals that received the muscle injury only), sections were obtained from the locations that corresponded to those in the bones with defects.

Identification of the Cells of Bone

A system for identification of pertinent cell types based on morphologic and histochemical properties was adopted.[3,18,21,22] (Fig 2). Briefly, cambial cells are alkaline phosphatase positive cells with a spindle shaped, darkly staining nucleus, typically 5 × 10 μm, with scanty cytoplasm at 400×. Two phenotypes are distinguished on the basis of location and response to injury. Bone lining cells cover the bone surface and activate after injury to

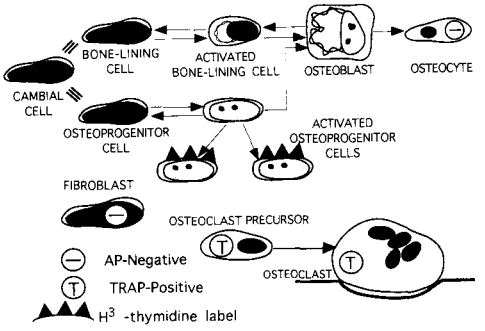

Fig 2. Schematic representation of functional relationships of the cells of bone. AP = alkaline phosphatase; TRAP = tartrate resistant acid phosphatase. All cell types are AP positive unless indicated otherwise (negative sign), except for the osteoclast (whose AP status was not ascertained).

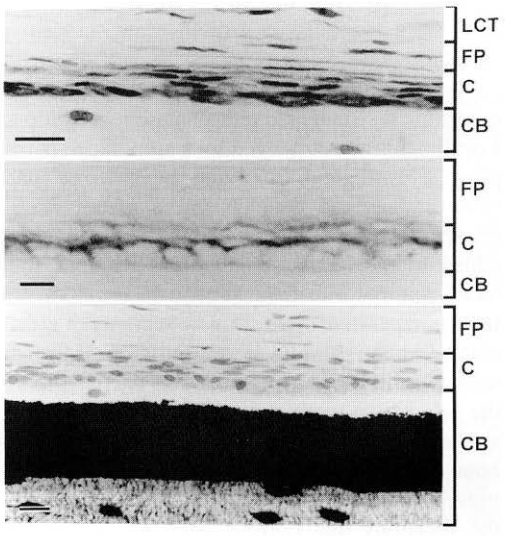

Fig 3. Representative photomicrographs of the resting periosteum. (Top) Toluidine-blue/basic-fuchsin; (middle) alkaline phosphatase (dark staining) was localized in the membranes of the cambial cells (van Gieson's). (Bottom) von Kossa, counterstained with nuclear fast red; the 80-μm dark staining band of cortical bone and the more superficial 20-μm nonstaining region were characteristic of noninjured bone. CB = cortical bone; C = cambium; FP = fibrous periosteum; LCT = loose connective tissue. Bars are 20 μm.

become osteoblasts without undergoing proliferation. An activated bone lining cell is identified by its uniform dark staining nucleus juxtaposed to a prominent Golgi apparatus. The osteoprogenitor cell is located above the bone lining cells; when activated, it exhibits a light staining nucleus with 1 to 2 nucleoli and then deactivates, divides, or differentiates into an osteoblast. The osteoblast is an alkaline phosphatase positive cell approximately 15 μm in its longest dimension, sometimes cuboidal, that contains a nucleus with nucleoli, extensive basophilic cytoplasm, and a prominent Golgi apparatus. The osteocyte is an alkaline phosphatase negative cell found in bone lacunae, and the osteoclast is a tartrate resistant acid phosphatase positive, multinucleated cell located on a bone surface. The fibroblast is an alkaline phosphatase negative cell found in the fibrous periosteum and loose connective tissue; it is morphologically indistinguishable from the cambial cell.

Quantitative Measurements

Quantitative measurements were made within ±3 mm from the center of the defect; in the tibiae that lacked the defect, the 6-mm length was centered in the region of interest. Proliferation was assessed by counting the number of cells with 5 or more grains per nucleus, because preliminary studies demonstrated that this concentration was sufficient to distinguish a proliferating cell from background (a concentration of 5 grains was not encountered except over a nucleus). Labeled cells were counted in the cambium, fibrous periosteum, loose connective tissue, and within the defect; the counts were normalized by the length of the cortical bone surface along which the labeled cells were located, and the value used in all subsequent calculations was the mean of the 3 representative sections, expressed as cell count per millimeter of bone. The quantitative results were expressed as a cell linear density rather than a ratio of the number of 2 cell types (the mitotic index, for example), as in previous studies,[14,26] because cell ratios contain 2 parameters that can be confounded by the experimental manipulations. The distance of each labeled cell in the cambium above the intact cortical bone surface was also measured.

Differentiation was assessed by counting the number of osteoblasts in the cambium and within the defect in methyl-green/thionin stained sections; an osteoblast was identified as a cell containing a green nucleus, a prominent but unstained Golgi, and purple cytoplasm; all 3 features were required before accepting a particular cell as an osteoblast. The osteoblast count was also normalized to the length of the bone surface and was expressed as the number of osteoblasts per millimeter of bone. As described previously, the results were averaged over 3 sections, and the mean was used in all statistical evaluations.

Periosteal callus thickness was measured from the original bone surface to the superficial edge of the callus at 200-μm intervals along the cortical surface. Within the defect, the average area fraction of callus was measured and expressed as a fractional volume within the defect.[1] All morphometric length and area measurements were made using a computer based system (Bioquant System IV, R&M Biometrics, Nashville, TN). The data were evaluated by means of the unpaired t-test at $p < 0.05$.

RESULTS

The Resting Periosteum

The typical appearance of the resting periosteum in noninjured bone is shown in Figure 3; the periosteum was 20 ± 10 μm thick and contained 2 to 5 layers of cells. The fibroblast, which predominated in the fibrous periosteum (20 ± 15 μm) and the loose connective tissue, was easily distinguished from cambial cells by the absence of alkaline phosphatase in the cell membrane. The fibrous periosteum blended into the loose connective tissue, which was characterized by a lack of fiber orientation. The cortical bone was 800 μm thick and contained a von Kossa positive strip on the periosteal surface; the stain also penetrated into the adjacent vascular channels, lacunae, and canaliculi. Proliferating cells were rare in the cambium (0.3 ± 0.1 cells/mm), and no tartrate resistant acid phosphatase positive cells were present. Areas of localized bone formation were seen occasionally along the bone surface, consisting of a single layer of osteoblasts on the cortical surface. In these instances, the cambial cells superficial to these osteoblasts were activated, as evidenced by plump nuclei containing nucleoli.

The Healing Response

The healing pattern is illustrated schematically in Figure 4, and representative photomicrographs are shown in Figures 5, 7, 9, 10, 12, 13, and 14; quantitative data are presented in Figures 6, 8, 11, and 15.

One Day After Injury

Clot containing inflammatory cells and von Kossa positive bone debris filled the bone defect and extended into the loose connective tissue; a thin von Kossa positive band of cortical bone was present along the bottom of the defect, but elsewhere, the thicker band characteristic of noninjured bone was present (Fig 5). Increased proliferation was observed in the cambium, fibrous periosteum, and loose connective tissue superficial to the uninjured cortical surface within the region of interest but was not seen in the clot (Fig 6).

Fibrous periosteum was missing or displaced from the cortical surface up to 500 μm from the defect margin (Fig 7, top), resulting in a denuded layer of alkaline phosphatase positive resting cambial cells 1 to 2 cells deep; further from the site, the fibrous periosteum was intact and most of the cambial cells were activated. Osteoblasts were seen on a narrow strip of osteoid (typically, 10 μm) on the cortical bone (Fig 7, bottom) but not in a concentration that was significantly different from baseline levels (Fig 8). The osteoblasts did not contain tritiated thymidine, indicative of their derivation from the bone lining cells. Proliferating osteoprogenitor cells and fibroblasts were present above the osteoblasts (Fig 6). At 5 to 6 mm beyond the defect, the periosteum was largely indistinguishable from the resting periosteum.

Two Days After Injury

The fibrous periosteum was reattached to the bone surface at the margin of the defect, resulting in segregation of the cambial compartment from the clot and loose connective tissue (Fig 9). Proliferation in the cambium, fibrous periosteum, and loose connective tissue was the greatest observed in the study (Fig 6). Activated osteoprogenitor cells and osteoblasts were present along the bone surface except within 500 μm of the defect, where the cells were still morphologically similar to resting cambial cells. The response to muscle injury resulted in significantly less proliferation compared with bone injury (Fig 10).

The proliferation in the cambium resulted in a periosteum that reached 100 μm at its thickest point (1 mm from the defect edge), which included 20 to 40 μm of osteoid that was laid on the cortical bone. The newly deposited osteoid progressively displaced the location of the proliferating cambial cells from the cortical surface (Fig 11). Osteoblasts, blood vessels, and patches of osteoid were seen above the cortical osteoid. The osteocytes within the osteoid were large, and their lacunae were irregularly

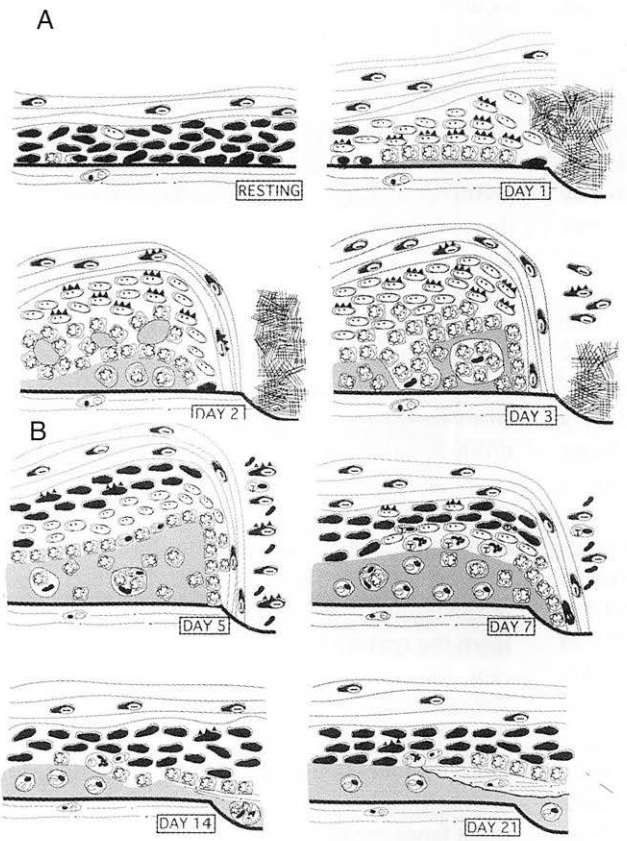

Fig 4A–B. (A) Schematic representation of the resting periosteum and the general histologic features of the response 1 to 3 days after a surgically induced defect (blind hole). The response was symmetric about the defect, consequently, only half of the response (and the defect) is shown. Cross hatching indicates clot. The cellular icons are defined in Figure 2 except for the erythrocytes. (B) Schematic representation of the general histologic features of the periosteum 5 to 21 days after a surgically induced defect (blind hole).

shaped and lacked orientation compared with osteocytes in the original cortical bone. The superficialmost cambium stained intensely for alkaline phosphatase (Fig 12) and contained many proliferating osteoprogenitor cells. Beyond 3 mm from the defect margin, activation of osteoprogenitor cells was seen but proliferation was low; the bone surface was covered with about 10 μm of osteoid.

Three Days After Injury

Osteoprogenitor cells adjacent to the bone defect were activated, and osteoblasts and osteoid were present on the bone surface at the defect margin where the fibrous periosteum was missing previously. Proliferation was increased in all tissue compartments, including the defect (Fig 6); the periosteum nearer the defect was particularly active. The patches of osteoid and cortical osteoid that were evident on Day 2 coalesced to form periosteal callus.

Alkaline phosphatase localization was greatest in the superficial cambium and within the osteoid spaces (Fig 12); the osteoblast like osteocytes encased in the new osteoid were moderately stained, suggesting a change toward an alkaline phosphatase negative phenotype. Within 100 μm of the original bone surface, the osteocytes were morphologically similar to osteoblasts, but the matrix stained lightly or not at all for alkaline phosphatase.

Within the osteoid, von Kossa positive fingerlike formations radiated from the von Kossa positive cortical bone surface (Fig 5) and surrounded the osteocytes within the osteoid. Tartrate resistant acid phosphatase negative giant cells were present on the surface of the von Kossa positive bone remnants.

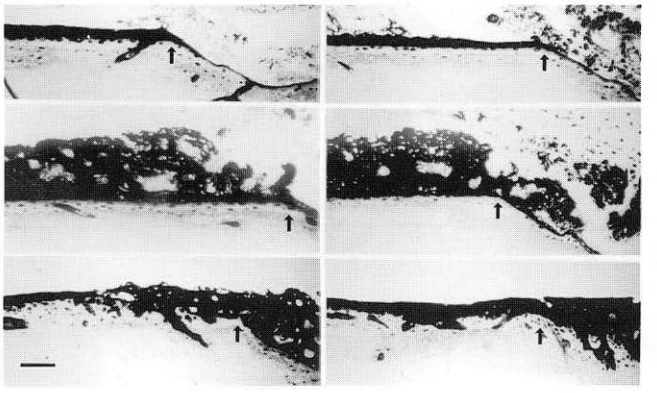

Fig 5. The time dependent response to injury as manifested in von Kossa stained sections. The bone defect is on the right (arrows). From left to right and top to bottom, 1, 3, 5, 7, 14, and 21 days after injury, respectively. The bar (lower left) is 200 μm. At Day 1, the staining of the intact cortical surface was similar to that seen in uninjured bone; the bone surface in the defect stained poorly, except where the stain entered vascular channels. The von Kossa positive material in the soft tissue is bone debris. By Day 3, regions immediately superior to the original cortical surface became von Kossa positive, indicating that mineralization had occurred in these areas. By Day 5, almost all of the osteoid was mineralized. Thereafter, the callus was modeled.

Five Days After Injury

A dense layer of collagen capped the granulation tissue that filled the injury site; the layer fused with the fibrous periosteum on both sides of the defect. Proliferation was high in the granulation tissue that filled the defect but was reduced elsewhere in the loose connective tissue and throughout the region of interest (Fig 6). No evidence of cortical bone degeneration at the defect site was seen. The defect was largest at the time of surgery and became progressively smaller with time, beginning on Day 5. Bone debris created during the injury was removed by phagocytes and tartrate resistant acid phosphatase negative giant cells, but the original (preinjury) bone was not subjected to any catabolic activity. Thus, bone necrosis that is believed to occur at the ends of fracture fragments in some cases[8] is not an essential feature of bone healing, at least for injuries of the type studied here.

Osteoblasts were seen for the first time within the defect (Fig 8B). Tartrate resistant acid phosphatase positive mononuclear cells appeared in the granulation tissue, in the superficial cambium, and within the osteoid spaces of the cambium.

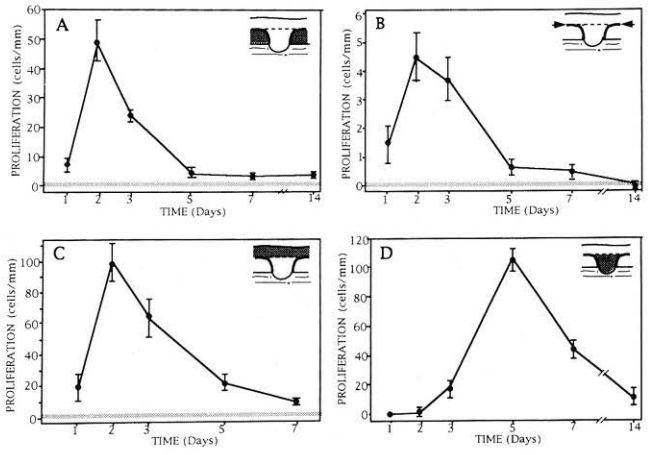

Fig 6A–D. Proliferative response in the indicated (dark shading or arrows) compartments of the region of interest. Baselines (light shading) were determined from 10 control rats (20 tibiae). (A) Cambium (baseline, 0.3 ± 0.1 cells/mm). (B) Fibrous periosteum (0.1 ± 0.1 cells/mm). (C) Loose connective tissue (0.4 ± 0.1 cells/mm). (D) Within the injury site. Each point is the mean ± standard error of the mean from 5 rats. All values shown were statistically elevated above baseline ($p < 0.05$), except for Day 14 in the fibrous periosteum. The cells were positive for alkaline phosphatase in A but negative in B and C; both phenotypes were present in D.

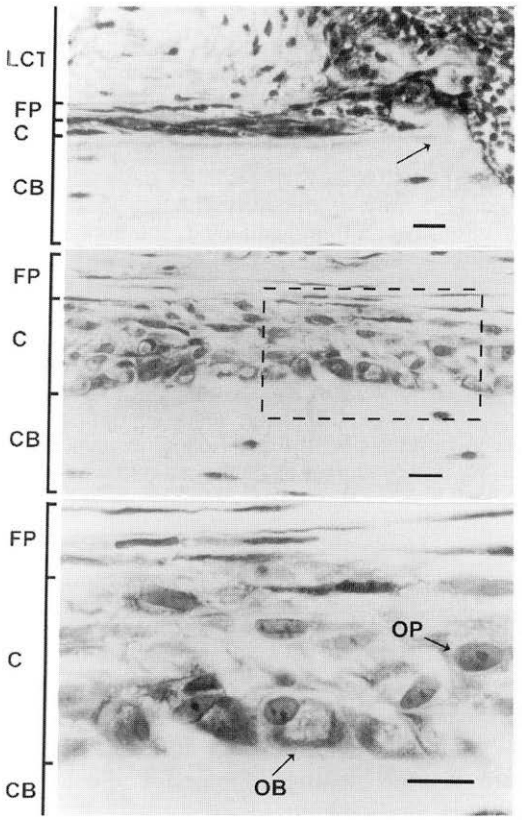

Fig 7. The periosteum in relation to the bone defect 24 hours after injury. (Top) The fibrous periosteum was absent at the defect margin (arrow); extravasated blood was present among the (inactive) cambial cells. (Middle) Farther from the defect the periosteum was intact, and the cambium was activated. (Bottom) Higher magnification from the indicated region. Osteoblasts (OB) lined the bone surface and the predominant cell type within the cambium was the activated osteoprogenitor cell (OP). Toluidine-blue/basic-fuchsin. CB = cortical bone; C = cambium; FP = fibrous periosteum. Bars are 20 μm.

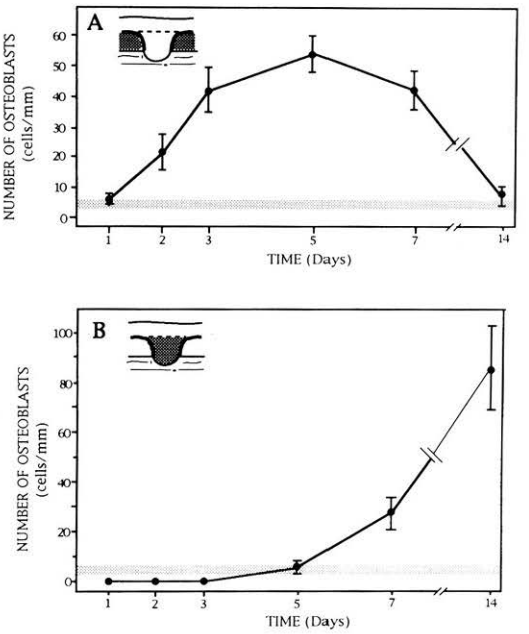

Fig 8A–B. Osteoblast concentration in the indicated (dark shading) regions in the region of interest following injury. (A) The region not containing the bone defect. Baseline (light shading) 4.7 ± 0.6 cell/mm from 10 rats (20 tibiae); all values were significantly elevated above baseline ($p < 0.05$) except for Days 1 and 14. (B) In the bone defect. Each point is the mean (± standard error of the mean) of 5 rats.

Except for some osteoid adjacent to the fibrous periosteum, the new matrix was von Kossa positive (Fig 5), indicating that it had calcified. The resulting periosteal callus was present along the entire length of the cortical bone up to the defect margin. The new matrix was thickest (200 μm) within 1 mm of the defect margin. Alkaline phosphatase was present in the cells located between the superficial edge of the callus and the fibrous periosteum, but the new matrix and its osteocytes were alkaline phosphatase negative except for the larger spaces within the periosteal callus, which were still lined with alkaline phosphatase positive osteoblasts (Fig 12). Many of the cells within the cambium were similar to resting cambial cells, resulting in a less distinct border between the fibrous periosteum and cambium compared with Day 3. Above the osteoblasts that lined the superficial edge of the callus were resting cambial cells. Proliferation throughout the cambium was reduced but remained above that of noninjured tissue.

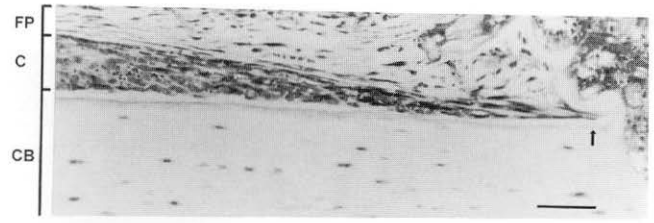

Fig 9. Attachment of the fibrous periosteum to the bone surface near the defect margin (arrow) 2 days after injury. Toluidine-blue/basic-fuchsin. Bar is 50 μm.

Seven Days After Injury

Osteoid appeared at the margins of the defect in scanty amounts. Tartrate resistant acid phosphatase positive mononuclear cells were present within the granulation tissue and within the spaces of the periosteal callus, and modeling of mineralized osteoid by osteoclasts was seen (Fig 13). Baseline proliferation was seen in all areas except the defect.

Adjacent to the injury site, the fibrous periosteum was highly cellular and in some areas was completely obscured by cells. A thin layer of alkaline phosphatase positive cells covered the surface of the periosteal callus, but the callus itself was negative for alkaline phosphatase (Fig 12). Resorption had occurred, as evidenced by areas of irregular bone surface; tartrate resistant acid phosphatase positive osteoclasts were located in Howship's lacunae on the bone surface within 1 to 1.5 mm of the defect edge, and extracellular tartrate resistant acid phosphatase was evident next to the osteoclasts. Acid phosphatase negative giant cells were also present.

Mean callus formation in the bone and muscle injured groups is shown in Figure 15; a lateral to medial gradient in callus formation was observed in the latter group.

Fourteen Days After Injury

Callus filled the peripheral areas of the defect, but the core contained only fibrous tissue (Fig 14). A thin alkaline phosphatase positive layer of cambial cells covered the bone surface (Fig 12). Farther from the defect, the periosteum resembled that of noninjured tissue. Localized areas of resorption were evident at the defect margins, and in some animals the periosteal callus directly adjacent to the defect was resorbed. A thick, fibrous band, probably the collapsed cap of the granulation tissue and the fibrous periosteum, was seen over the defect.

Adjacent to the defect, the von Kossa staining of the new periosteal bone was irregular (Fig 5). Tartrate resistant acid phosphatase positive osteoclasts and extracellular tartrate resistant acid phosphatase were present within the defect.

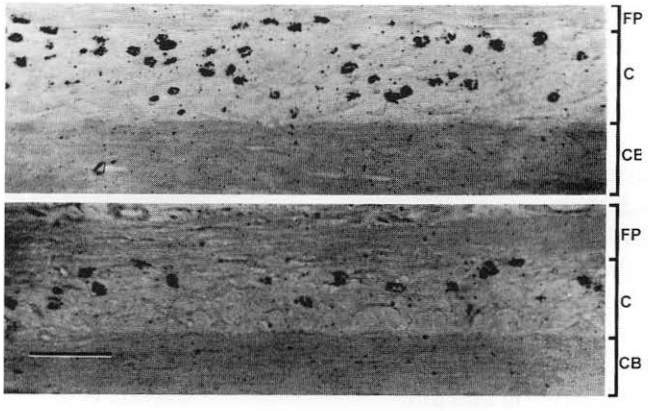

Fig 10. Proliferative response 2 days after injury. (Top) A rat that received the bone defect. Elevated proliferation occurred in all tissue compartments (see Fig 6). (Bottom) Proliferation in a rat that received only a soft tissue injury (removal of 10% of the anterior tibialis muscle) at the corresponding anatomic location. Autoradiograph/van Gieson's. CB = cortical bone; C = cambium; FP = fibrous periosteum. Bar is 100 μm.

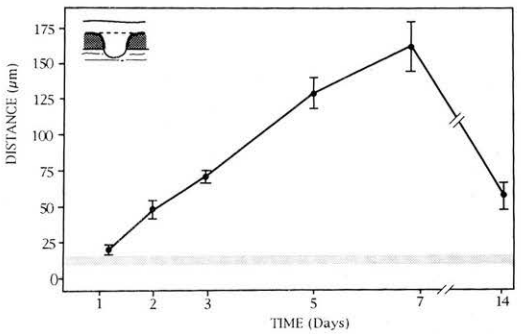

Fig 11. Distance of proliferating cambial cells above the cortical surface in the portion of the region of interest that did not include the defect (dark shading). Each datum point is the mean ± standard error of the mean for 5 rats. Baseline (light shading), 12.9 ± 1.6 μm, from 10 rats (20 tibiae). All values were significantly elevated above baseline ($p < 0.05$) except for Day 1. The increase resulted from increased cellularity and the formation of osteoid on the original cortical surface, which progressively displaced the osteoprogenitor cell compartment.

Twenty-One Days After Injury

The bone surface was restored, and the defect was filled with woven bone (Figs 14 and 15). The alkaline phosphatase positive cambial layer superficial to the defect and along the length of bone was similar to that in noninjured bone. On the bone surface above the filled defect was a single layer of osteoblasts that, in some areas, extended beyond the width of the defect. Only a few tartrate resistant acid phosphatase positive osteoclasts and tartrate resistant acid phosphatase positive mononuclear cells were present on the bone surface and within the loose connective tissue, and overall tartrate resistant acid phosphatase staining was reduced.

The new bone within the defect and on the surface of the original cortical bone surface was woven bone; it was capped by a layer of appositional bone (Fig 14) within which the osteocytes were located in almond shaped lacunae oriented parallel to the cortical bone surface. The appositional bone was von Kossa positive (Fig 5), as in noninjured bone. Sporadically throughout the study, small isolated areas of cartilage were occasionally seen.

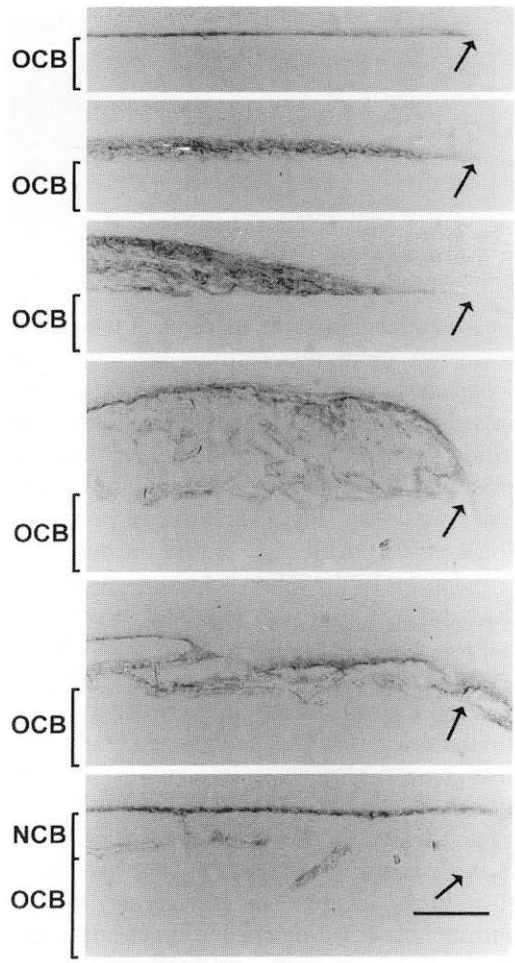

Fig 12. Alkaline phosphatase localization (dark staining) after injury to bone (counterstained with van Gieson's). From top to bottom, 1, 2, 3, 5, 7, and 14 days after injury, respectively. At 1 day, the alkaline phosphatase positive cambial layer was similar to that in noninjured bone. At 2 days, it became thicker in the region away from the defect. On days 3 to 5, alkaline phosphatase positive cells were located in the superficial cambium and within the newly formed osteoid. Alkaline phosphatase positive cambial ingrowth into the defect occurred by Day 7 and subsequent modeling resulted in a pattern at Day 14 similar to that of noninjured bone. Arrows denote edge of defect. OCB = original cortical bone; NCB = new cortical bone. Bar is 200 μm.

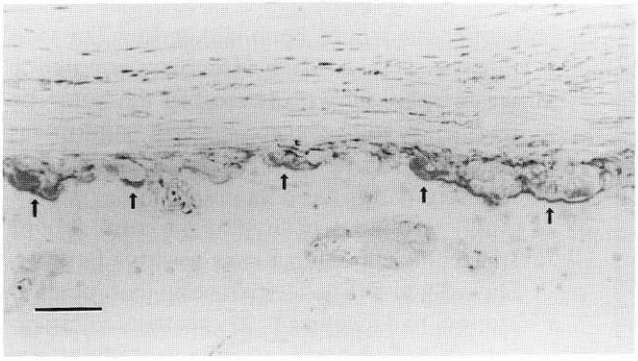

Fig 13. Localization of tartrate resistant acid phosphatase (dark staining, arrows) during resorptive phase of bone modeling at 7 days after surgery. Counterstained with methyl green. Bar is 200 μm.

DISCUSSION

Variance in healing in particular animal models has many causes, and elimination of 1 perturbing factor sometimes results in the occurrence of other such factors.[9,10,15,19,28] For example, movement at the injury site influences the healing cascade and tends to cause cartilage formation and delayed bony union. The effect of motion can be avoided by means of internal fixation, but implants affect the cellular response and can interfere with histomorphologic measurements. Drilling of holes in the cortex eliminates the need to stabilize the injury site, but such a model confounds the contributions to healing arising from the periosteum and the endosteum, making it difficult to assess mechanistic pathways. The model described in the current study minimized interanimal variability in the extent of the initial injury, isolated the cellular events that are essential in bone healing, facilitated assessment of the time dependent healing response, and permitted quantitative characterization of cell activity in terms of absolute parameters (cell densities).

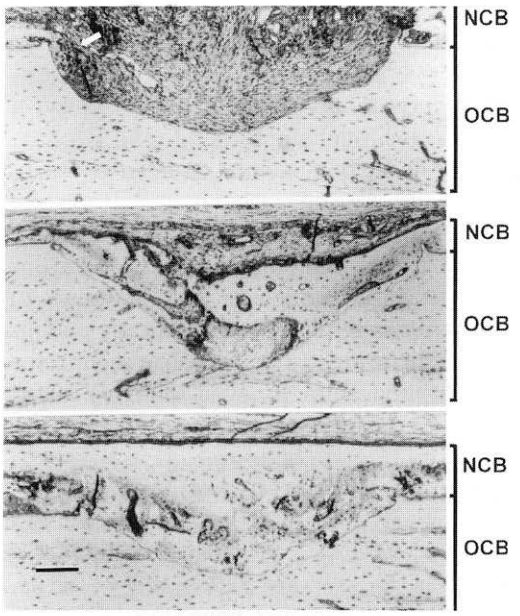

Fig 14. Bone formation at Days 7, 14, and 21 after injury. Toluidine-blue/basic-fuchsin. Scanty new bone was present in the defect at day 7 (arrow); healing was complete by Day 21. OCB = original cortical bone; NCB = new cortical bone. The bar is 200 μm.

Cambial proliferation increased after the injured fibrous periosteum became attached to the cortical surface at the defect margin (Fig 6A), thus isolating the cambium from the defect. Thereafter, osteoid grew from the cambium into the defect. These observations may indicate that regeneration of the fibrous periosteum and reestablishment of the cambial compartment was a necessary precondition for growth of osteoid into the defect. The connection between periosteal integrity and matrix synthesis in the defect, a relationship that has not been described in previous bone healing studies, suggests that the factors that regulated bone healing were confined to a spatially limited region that did not

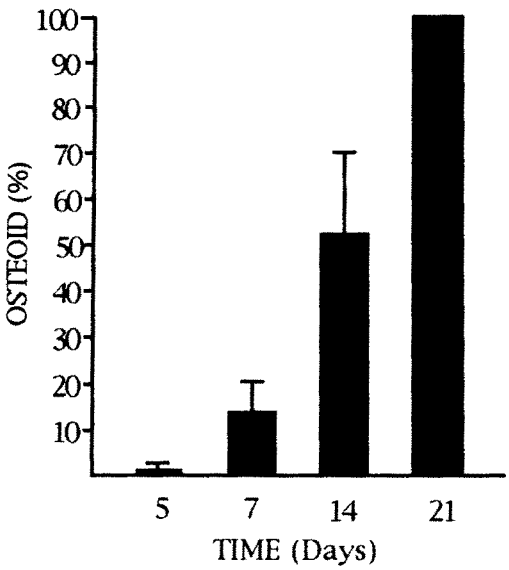

Fig 15. Bone formation in the defect at various times after injury. The mean (± standard error of the mean) fractional volume of the defect occupied by newly synthesized bone is shown (N = 5 at each time).

include, for example, clot, granulation tissue, bone debris, or leukocytes. If so, those factors may have been derived from the cambial cells or from the bone itself.

Additional evidence implicating the tibia as the source of the factors that regulated its healing was found in observations of osteoblastic activity. Three phenotypic osteoblast populations could be distinguished on the basis of cellular activity and location relative to the defect. First, woven osteoid produced by osteoblasts derived from bone lining cells formed on the cortical surfaces on each side of the defect where the fibrous periosteum was intact (Fig 4). By Day 2, osteoprogenitor cell proliferation and differentiation in the superficial region of the cambium produced osteoblast layers 3 to 4 cells deep on both sides of the defect that secreted woven osteoid interstitially in cords or patches superficial to the cortical osteoid; subsequently, the interstitial and cortical osteoid coalesced. After the callus at the defect margin was resorbed by osteoclasts, osteoblasts secreted appositional bone, which capped the woven bone laid earlier. The synthetic activity of each osteoblast population was symmetric with respect to the bone defect, suggesting that the healing pattern was at least partly determined by regulatory factors originating from the injury site.

The osteoid deposited on the cortical bone surface became von Kossa positive between Days 3 and 5 (Fig 5), indicating that mineralization had occurred. Thereafter, calcification followed matrix synthesis without any apparent delay. The reason for this apparently novel observation of delay in onset of mineralization is unknown; one possibility is that the chemical dynamics of the interstitial Ca^{2+} and PO_4^{-3} were altered during clot removal, which also occurred between Days 3 to 5, thereby favoring precipitation of hydroxyapatite.[20]

An example of the use of the model for evaluation of the differential effect of injury to bone versus soft tissue is shown in Figure 10. The proliferative response in the cambium 2 days after bone injury (Fig 10, top) was 49.5 ± 7.2 cells/mm (Fig 6A); in the rats that received only the soft tissue injury, it was 9.2 ± 3.8 cells/mm ($p < 0.05$). Because the soft tissue damage and associated vascular disruption and inflammatory response was significantly greater in the case of the muscle injury compared with the bone injury, the result suggests that an injury to bone itself is required to explain the magnitude of the proliferative response seen in the bone injured animals, even though a weak mitogenic factor was produced by a soft tissue injury (Fig 10, bottom).

During Days 5 to 14 postinjury, the defect progressively filled with new bone as a result of centripetal growth from the defect margins; at Day 14, for example, 53% ± 17% of the defect was filled with new bone (Fig 15). When the fractional volume of new callus was computed using 7 equally spaced sections through the defect (instead of 3), the result was 56.3% ± 5.8%. This relatively low standard error indicates that measurements on 7 sections in

each of 5 animals would provide a reasonable likelihood of detecting changes in fractional volume due to experimental treatment. Thus, regardless of whether small differences are biologically significant, the model is suitable for hypothesis testing regarding factors that regulate bone growth.

Giant cells were seen as early as the third day after injury; osteoclasts, however, were not observed until the seventh day after injury, at which time they appeared on the surface of the newly mineralized callus. On the basis of observations made thus far, it appears that the disappearance of the clot, the mineralization of the callus, and the appearance of osteoclasts were simultaneous, suggesting that these events may have been related. Perhaps removal of the clot altered the local pH, resulting in chemical dynamics that favored precipitation of inorganic crystals, which, in turn, created an environment conducive to osteoclasts.

The appearance of osteoclasts could also be related to the appearance of the newly differentiated osteoblasts, because the osteoclasts did not appear at the injury site until after osteoid was secreted; they appeared precisely at the site of maximum osteoblastic synthetic activity, suggesting that the osteoclast recruitment factor came from the osteoblasts. Expression of the osteoblast phenotype involves a temporal pattern of gene expression that begins with activation of the genes that encode extracellular matrix, followed by downregulation of the matrix genes and upregulation of gene expression associated with preparation of the matrix for mineralization.[25] The osteoblast gene products related to mineralization may constitute the signal that results in the recruitment of osteoclasts; alternatively, the osteoclast signal may be derived from chemical, physical, or electrical consequences of mineralization.

Knowledge of the cellular basis of bone healing is needed to effectively manage the normal response and to appropriately treat pathologic cases. The animal model developed in the current study is potentially useful because it permits quantitative characterization of the time-dependent changes that occur after injury. Thus, the model is suitable for studying various questions, such as the role of soft tissue injury in the response of bone cells and the regulatory role of various factors, including hormones and cytokines, that have been suggested as regulatory agents on the basis of cellular studies.

References

1. Aherne WA, Dunnill MS: Morphometry. London, Edward Arnold Publishers 1982.
2. Anderson C: Manual for the Examination of Bone. Boca Raton, CRC Press 1982.
3. Aubin JE, Turksen K, Heersche JN: Osteoblastic Cell Lineage. In Noda M (ed). Cellular and Molecular Biology of the Bone. New York, Academic Press 1–45, 1993.
4. Bassett CA, Mitchell SN, Gaston SR: Treatment of ununited tibial diaphyseal fractures with pulsing electromagnetic fields. J Bone Joint Surg 63A: 511–523, 1981.
5. Brighton CT, Black J, Friedenberg ZB, et al: A multicenter study of the treatment of non-union with constant direct current. J Bone Joint Surg 63A:2–13, 1981.
6. Brighton CT, Schaffer JL, Shapiro DB, Tang JJ, Clark CC: Proliferation and macromolecular synthesis by rat calvarial bone cells grown in various oxygen tensions. J Orthop Res 9:847–854, 1991.
7. Burstone MS: The relationship between fixation and techniques for the histochemical localization of hydrolytic enzymes. J Histochem Cytochem 6:322–339, 1958.
8. Cornell CN, Lane JM: Newest factors in fracture healing. Clin Orthop 277:297–311, 1992.
9. Einhorn TA, Simon G, Devlin VJ, et al: The osteogenic response to distant skeletal injury. J Bone Joint Surg 72A:1374–1378, 1990.
10. Enneking WF: The repair of complete fractures of rat tibias. Anat Rec 101:515–538, 1948.
11. Gruber HE, Marshall GJ, Nolasco LM, Kirchen ME, Rimoin DL: Alkaline and acid phosphatase demonstration in human bone and cartilage: Effects of fixation interval and methacrylate embedments. Stain Technol 63:299–306, 1988.
12. Gundberg CM, Markowitz ME, Mizruchi M, Rosen JF: Osteocalcin in human serum: A circadian rhythm. J Clin Endocrinol Metab 60:736–739, 1985.
13. Heckman JD, Ryaby JP, McCabe J, Frey JJ, Kilcoyne RF: Acceleration of tibial fracture-healing by non-invasive, low-intensity pulsed ultrasound. J Bone Joint Surg 76A:26–34, 1994.
14. Kember NF: Cell populations kinetics of bone growth: The first ten years of autoradiographic studies with tritiated thymidine. Clin Orthop 76:213–230, 1971.

15. Kirkeby OJ, Ekeland A: No effects of local somatomedin C on bone repair. Continuous infusion in rats. Acta Orthop Scand 63:447–450, 1992.
16. Küntscher G: The Callus-Problem. (Altner PC, Translator). St Louis, Warren H. Green 1974.
17. Liu C, Sangvi R, Burnell JM, Howard GA: Simultaneous demonstration of bone alkaline and acid phosphatase activities in plastic-embedded sections and differential inhibition of the activities. Histochemistry 86:559–565, 1987.
18. Miller SC, Jee WS: The bone lining cell: A distinct phenotype? Calcif Tiss Int 41:1–5, 1987.
19. Mueller M, Schilling T, Minne HW, Ziegler R: A systemic acceleratory phenomenon (SAP) accompanies the regional acceleratory phenomenon (RAP) during healing of a bone defect in the rat. J Bone Miner Res 6:401–410, 1991.
20. Neuman WF, Neuman MW: The Chemical Dynamics of Bone Mineral. Chicago, University of Chicago Press 1958.
21. Owen M: The origin of bone cells in the postnatal organism. Arthritis Rheum 23:1073–1080, 1980.
22. Pritchard JJ: Histology of Fracture Repair. In Clark JM (ed). Modern Trends in Orthopaedics. Vol 4. London, Butterworths 69–90, 1964.
23. Rogers AW: Techniques of Autoradiography. New York, Elsevier 1979.
24. Sevitt S: Bone Repair and Fracture Healing in Man. New York, Churchill Livingstone 1981.
25. Stein GS, Lian JB, Owen TA: Relationship of cell growth to the regulation of tissue-specific gene expression during osteoblast differentiation. FASEB J 4:3111–3123, 1990.
26. Tenenbaum HC, McCulloch CA, Palangio K: Simultaneous autoradiographic and histochemical analysis of bone formed in vitro. J Histochem Cytochem 34:769–773, 1986.
27. Tripp EJ, MacKay EH: Silver staining of bone prior to decalcification for quantitative determination of osteoid in sections. Stain Technol 47:129–136, 1972.
28. Urist MR, McLean FC: Calcification and ossification: I. Calcification in the callus in healing fractures in normal rats. J Bone Joint Surg 23:1–16, 1941.